

Removal of malachite green in aqueous solution by adsorption on sawdust

Yinghua Song[†], Shenguang Ding, Shengming Chen, Hui Xu, Ye Mei, and Jianmin Ren

Department of Chemistry and Chemical Engineering, Chongqing Key Lab of Catalysis & Functional Organic Molecules, Chongqing Technology and Business University, Chongqing 400067, China

(Received 26 September 2014 • accepted 16 May 2015)

Abstract—A new adsorbent was synthesized from sawdust, a forest residue, in which methanol was used as a solvent and triethylamine as a modification agent under the following optimum conditions: 25 °C of reaction temperature, 1 : 8.75 of the ratio of sawdust to triethylamine (g : mL) and 1 hour of reaction time. The adsorption capacity of this adsorbent for malachite green was improved by 632.98% in contrast to that of the unmodified sawdust under the same adsorption conditions. Factors affecting the adsorption behavior of this adsorbent for malachite green, such as pH value, adsorption time, temperature and initial dye concentration, were evaluated through experiments in a batch system. The results indicated that the maximum adsorption capacity can be achieved at 5.08 of pH value and adsorption equilibrium can be reached in 6 hours. It was also found that the higher the temperature, the higher the adsorptive capacity would be. The Freundlich isotherm model provides a better description for the adsorption equilibrium when compared with the Langmuir equation in the conditions of the present study. Additionally, to examine the controlling mechanisms of the process, kinetic equations of the mass transfer and chemical reaction, the pseudo-first order model, the pseudo-second order model and the intraparticle diffusion model were used to correlate the experimental data respectively. The adsorption process of malachite green on sawdust tended to be controlled simultaneously by film mass transfer and intra-particle diffusion and it accompanied chemical reactions. It showed that the sawdust modified with triethylamine had good performance for cationic dye and can be used as a biomass adsorbent to treat dyes-containing wastewater with high quality.

Keywords: Sawdust, Triethylamine, Adsorption, Malachite Green

INTRODUCTION

Synthetic dyes are widely used in various industries, such as textile, paper, leather, plastic, printing and cosmetics, and their colored products. The discharged colored wastewater can pose a great threat to human health due to its toxicity and carcinogenicity [1,2]. Such effluent must be treated before being discharged into the environment. But many synthetic dyes are difficult to degrade because of their complex aromatic species and xenobiotic properties. Malachite green (MG) is an important cationic dye belonging to the triphenylmethane family, and it is widely used in color wool, silk, cotton and leather products. It's also used as fungicide and disinfectant in the fish farming industry, aquaculture and animal husbandry. It has been shown that MG may cause increasing risk of cancer and many other diseases due to its carcinogenic and mutagenic characteristics.

Many physical and chemical processes are available to remove dyes, such as advanced oxidation, combined chemical and biochemical process, adsorption membrane filtration, aerobic and anaerobic digestion. Activated carbon works as adsorbent to remove dyes in the wastewater in most commercial systems because of its high adsorption ability, but the processing costs are still expensive. So people try to develop cheaper and more effective adsorbents to re-

move dyes and find an alternative method from different starting materials such as bagasse pith [2], sawdust [3], rice husk [4,5], fly ash [6], melon husk [7], potato peel [8], hen feather [9], polar leaf [10], walnut shell [11], papaya seed [12], clay [13], peanut husk [14], *Trapa bispinosas*' peel and fruit [15], and pine cone powder [16].

The objectives of this work were to introduce a new adsorbent from sawdust chemically modified with triethylamine to investigate the adsorption of MG on it with respect to initial dye concentration, pH value and temperature, to gain equilibrium data of the MG adsorption on sawdust, and to discuss the kinetic parameters and intraparticle diffusion models of MG adsorption on sawdust.

MATERIALS AND METHODS

1. Preparation of Chemically Modified Sawdust (CMS)

Sawdust samples, derived from cypress trees, were obtained from a local carpentry workshop in Chongqing, Rep. of China. The sawdust was first washed copiously with distilled water to remove dust and impurities and dried at 60 °C in an air circulating oven. For uniform modification and reproducible results, the sawdust was then sieved into 40-60 meshes before modification. Sawdust (1.0 g) was mixed with 10 mL of triethylamine in methanol (10 mL), then the mixture reacted for 0.5 h at room temperature. The chemically modified sawdust (CMS) was rinsed with distilled water to remove residual materials and then oven-dried and stored in a desiccator.

2. Chemicals

Stock solution of MG (500 mg·L⁻¹) was prepared by dissolution

[†]To whom correspondence should be addressed.

E-mail: yhswjyhs@126.com

Copyright by The Korean Institute of Chemical Engineers.

of MG in twice-distilled water. The test solutions were prepared by diluting the stock solution to the desired concentration. All reagents were analytical reagent grade and used without further purification. The initial pH was adjusted to the pre-determined value (2.00-12.00) ± 0.10 using NaOH or HCl solutions prior to addition of adsorbent.

3. Batch Adsorption Studies

A volume of 100 mL of MG solutions at the desired concentration was introduced into 150 mL conical flasks. 0.01 g of CMS was added to the solutions. The flasks were agitated on a shaker at 150 rpm at constant temperature. Samples were taken from the mixture during stirring at predetermined time intervals to determine the residual MG concentration in the system. Samples were centrifuged and the supernatant liquid was analyzed for the remaining color. All the experiments were carried out twice in parallel and average values were calculated further. For isotherms studies, a series of flasks containing 100 mL of MG solution in the range of 40-360 $\text{mg}\cdot\text{L}^{-1}$ were prepared. CMS (0.01 g) was added to each flask and then the mixtures were agitated at 25, 30, 35, 40 and 45 °C, respectively, for 6 h.

The adsorption capacity q ($\text{mg}\cdot\text{g}^{-1}$) was calculated as follows:

$$q = \frac{v(c_0 - c_t)}{m} \quad (1)$$

where c_0 and c_t are the initial concentration and the concentrations at t moment ($\text{mg}\cdot\text{L}^{-1}$); v is the volume of MG solution used (L); and m is the mass of the dry CMS used (g).

4. Analysis

The concentration of residual MG in the adsorption system was determined spectrophotometrically (UV1102 spectrophotometer, TECHCOMP, China). The absorbance of the color was measured at 616 nm.

5. Adsorption Isotherms and Thermodynamic Parameters

Langmuir and Freundlich isotherms are the most widely used isotherms since they can be applied to a wide range of adsorbate concentrations. The linear form of the Langmuir equation is generally accepted in the following variation:

$$\frac{c_e}{q_e} = \frac{1}{K_L q_{max}} + \frac{c_e}{q_{max}} \quad (2)$$

where c_e is the equilibrium concentration of dye solution ($\text{mg}\cdot\text{L}^{-1}$), q_e is the equilibrium capacity of dye on the adsorbent ($\text{mg}\cdot\text{g}^{-1}$), q_{max} is the maximum monolayer adsorption capacity of the adsorbent ($\text{mg}\cdot\text{g}^{-1}$), and K_L is the Langmuir adsorption constant ($\text{L}\cdot\text{mg}^{-1}$).

The Freundlich isotherm equation is a semi-empirical one employed to describe a heterogeneous system:

$$\ln q_e = \ln k_f + \frac{1}{n} \ln C_e \quad (3)$$

where k_f ($\text{L}\cdot\text{mg}^{-1}$) and n (dimensionless) are the Freundlich adsorption isotherm constants, indicating the capacity and intensity of the adsorption, respectively.

6. Adsorption Kinetics

To examine the controlling mechanism of adsorption processes such as mass transfer and chemical reaction, the pseudo-first order, pseudo-second order and intraparticle diffusion kinetic equations were used to correlate the experimental data. The pseudo-first order

kinetic model was suggested by Lagergren [17] for the adsorption of solid/liquid systems and its integrated form is given below:

$$\ln(q_e - q_t) = \ln q_e - k_1 t \quad (4)$$

where q_t ($\text{mg}\cdot\text{g}^{-1}$) was the adsorption capacity at time t (min^{-1}) and k_1 (min^{-1}) was the rate constant of the pseudo-first adsorption.

The kinetic data were further analyzed with Ho's pseudo-second order kinetics model [18] expressed as:

$$\frac{t}{q_t} = \frac{t}{q_e} + \frac{1}{k_2 q_e^2} \quad (5)$$

where k_2 ($\text{g}\cdot\text{mg}^{-1}\cdot\text{min}^{-1}$) is the rate constant of the pseudo-second-order adsorption.

The adsorption process generally follows three consecutive steps of external diffusion, intraparticle diffusion and actual adsorption. One or more of these steps control the adsorption kinetics altogether or individually. The kinetic data were also analyzed by intraparticle diffusion kinetics model [19] to determine the rate controlling step:

$$q_t = k_p t^{1/2} + C \quad (6)$$

where k_p ($\text{mg}\cdot\text{min}^{-1/2}\cdot\text{g}^{-1}$) is the intraparticle diffusion rate constant and C ($\text{mg}\cdot\text{g}^{-1}$) is a constant.

RESULTS AND DISCUSSION

1. Effect of Initial pH of Solution

The pH value of the solution is an important factor that must be considered in the adsorption process. The initial pH of the working solutions was adjusted between pH 2-12 by addition of diluting HCl and NaOH solution. The effect of pH on the adsorption of MG is shown in Fig. 1.

As shown in Fig. 1, a sharp increase in the adsorption capacity occurred as the pH of the initial solution increased from 2.0 up to 5.0, beyond which it remained a slow decrease. For the subsequent studies, pH 5.0 was selected as the optimal pH.

The lower removal of MG at lower pH is because of the presence of excess H^+ ions neutralizing negative charge at the surface

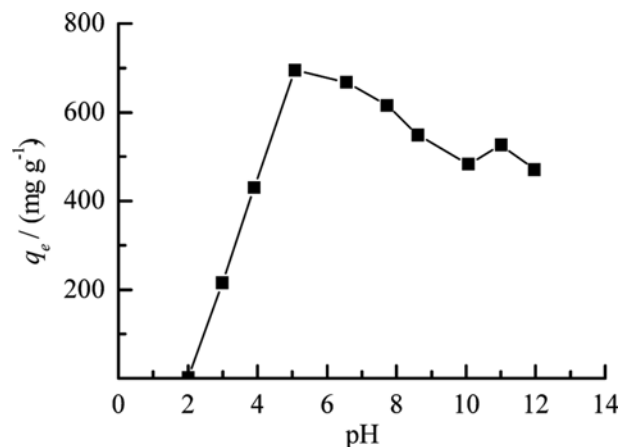


Fig. 1. Effect of pH on adsorption of MG on CMS ($T=25\text{ }^\circ\text{C}$, $c_0=100\text{ mg}\cdot\text{L}^{-1}$).

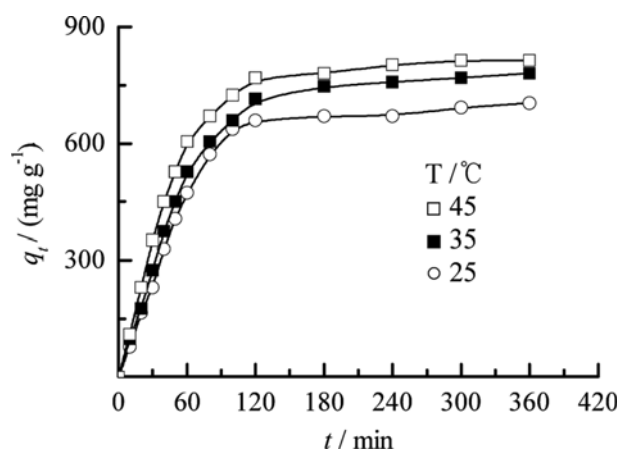


Fig. 2. Effect of contact time on adsorption of MG at different temperatures ($c_0=300 \text{ mg}\cdot\text{L}^{-1}$).

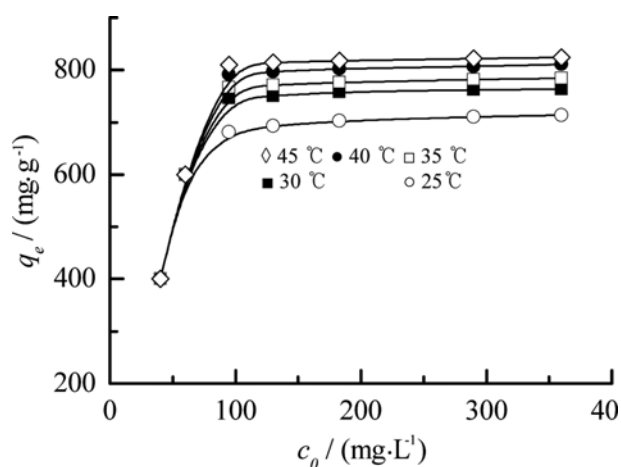


Fig. 3. Effect of initial dye concentration on the adsorption of MG on CMS at different temperatures.

of the CMS, which will inhibit the adsorption of cationic MG onto CMS. With pH increasing, protonation is reduced, and there will be more vacant negatively charged adsorption sites; the electrostatic attraction between the surface of CMS and positively charged cationic dye becomes dominant [16,20,21]. The blank test indicated that the pH value had significant effect on the color of MG itself. MG appears yellow when it is in strong acidic medium, and it turns colorless when in strong alkaline environment. The color is relatively stable when it is in weak acid solution. Therefore, when the pH is greater than 5.0, the alkaline condition may cause a change of the molecular structure of MG, and then the adsorption capacity shows a declining trend.

2. Effect of Contact Time

Removal of MG by CMS was performed with the dye concentration of $300 \text{ mg}\cdot\text{L}^{-1}$ at 25, 35 and 45°C , respectively. According to Fig. 2, there was an increase in equilibrium adsorption capacity at the same concentration when the temperature was higher. The adsorption capacity of CMS for MG increased from $703.30 \text{ mg}\cdot\text{g}^{-1}$ at 25°C to $813.19 \text{ mg}\cdot\text{g}^{-1}$ at 45°C due to its endothermic nature. The results also show that removal of MG was faster in initial 120 minutes and became slower and finally reached equilibrium at approximately 360 minutes. During initial stages, a large number of vacant sites were available on the surface of adsorbent and the adsorption of MG was very quick. Then the adsorption process became slower due to gradual occupancy of these sites. With increasing time, the occupation of the remaining vacant sites was more difficult due to increased repulsive forces between dye molecules and

bulk solution [12,16,22].

3. Effect of Initial Dye Concentration

The effect of initial dye concentration on the adsorption of MG by CMS at different temperatures is shown in Fig. 3. It is obvious that with the increase of the initial dye concentration the amount of MG adsorbed per unit mass of CMS increased. At lower concentrations, less than $60 \text{ mg}\cdot\text{L}^{-1}$, all MG present in the adsorption medium could combine with adsorption sites on the adsorbent surface. The increase of the loading capacity of CMS may contribute to the driving force provided by the high MG concentration to overcome all mass transfer resistance [22]. It may also be due to higher interaction between MG and adsorbent [22]. MG adsorption also showed a saturation trend at higher initial dye concentration while CMS offered a finite number of surface adsorption sites [8].

4. Adsorption Isotherms Parameters

The adsorption isotherm studies gave information about the capacity of adsorbent to remove dyes. Experimental adsorption equilibrium data in Fig. 3 obtained at different temperatures were fitted with Langmuir and Freundlich models. The isotherm constants, relative coefficients and standard deviations (SD) are tabulated in Table 1. The uncertainties of some parameters are also presented in Table 1. As observed, although the equilibrium data fitted well to both of the adsorption models, the Langmuir model exhibited a perfect fit to the adsorption data under the studied conditions due to extremely high relative coefficients and lower SD. The Langmuir model is based on a monolayer adsorption by the adsorbent

Table 1. Langmuir and Freundlich isotherm constants of MG on CMS at different temperatures

Temperature ($^\circ\text{C}$)	Langmuir				Freundlich			
	q_{\max} ($\text{mg}\cdot\text{g}^{-1}$)	K_L ($\text{L}\cdot\text{mg}^{-1}$)	R^2	SD (10^{-4})	n	k_f	R^2	SD (10^{-3})
25	719.42 ± 1.38	0.53 ± 0.08	1	5.86	51.75 ± 2.309	640.48 ± 2.71	0.9938	1.73
30	763.36 ± 0.84	1.19 ± 0.22	1	3.18	106.39 ± 7.73	724.37 ± 2.53	0.9818	1.57
35	787.40 ± 1.384	1.14 ± 0.29	1	4.93	120.51 ± 9.59	747.28 ± 2.54	0.9738	1.6
40	813.01 ± 2.25	1.11 ± 0.37	1	7.52	121.99 ± 11.61	772.85 ± 3.19	0.9689	1.99
45	826.45 ± 1.29	1.67 ± 0.50	1	4.17	172.41 ± 13.00	797.26 ± 1.69	0.9806	1.15

Table 2. Fitted parameters for different kinetic models

Model			Temperature/°C		
			25	35	45
First order kinetic	k_1 (10^{-2})	Rate constant, min^{-1}	2.05 ± 0.07	1.77 ± 0.04	1.98 ± 0.04
	$q_{e,cal}$	Equilibrium capacity, $\text{mg} \cdot \text{g}^{-1}$	839.4 ± 37.6	869.9 ± 20.7	881.4 ± 23.3
	R^2	Correlation coefficient	0.9898	0.9965	0.9975
	SD		0.069	0.037	0.041
Second order kinetic	k_2 (10^{-5})	Rate constant, $\text{g} \cdot \text{mg}^{-1} \cdot \text{min}^{-1}$	1.97 ± 0.23	1.94 ± 0.18	2.45 ± 0.28
	$q_{e,cal}$	Equilibrium capacity, $\text{mg} \cdot \text{g}^{-1}$	833.3 ± 44.1	909.1 ± 39.1	909.1 ± 25.4
	R^2	Correlation coefficient	0.9682	0.9797	0.985
	SD		0.025	0.018	0.015
Intraparticle diffusion	k_{p1}	Rate constant, $\text{mg} \cdot \text{min}^{-1/2} \cdot \text{g}^{-1}$	81.01 ± 3.76	83.68 ± 4.06	87.20 ± 5.69
	C_1	Intercept	-183.1 ± 28.3	-165.5 ± 30.5	-128.1 ± 42.8
	R_1^2	Correlation coefficient	0.9852	0.9838	0.971
	SD_1		27.29	29.45	41.31
	k_{p2}	Rate constant, $\text{mg} \cdot \text{min}^{-1/2} \cdot \text{g}^{-1}$	5.90 ± 1.73	5.92 ± 0.21	7.06 ± 1.66
	C_2	Intercept	589.2 ± 28.5	667.2 ± 3.5	689.7 ± 27.3
	R_2^2	Correlation coefficient	0.9944	0.9974	0.9502
	SD_2		7.18	0.89	6.87
$q_{e,exp}$	Experimental data of the equilibrium capacity, $\text{mg} \cdot \text{g}^{-1}$	738.5	819.2	853.8	

with the same energy of active sites. The surface of CMS was expected to have nearly homogeneous sites for MG adsorption; therefore, a much better fit was obtained [23,24]. The maximum monolayer capacity of CMS was determined as 719.42, 763.36, 787.40, 813.01 and 826.45 $\text{mg} \cdot \text{g}^{-1}$ for 25, 30, 35, 40 and 45 °C. The values of q_{max} increased with increasing temperature. The Freundlich constants, k_f , increased with increasing temperature and showed easy uptake of MG by the CMS. All n values were found to be greater than 1, which indicated a favorable adsorption condition in the process [8].

5. Kinetic Parameters of Adsorption

To investigate the adsorption process of MG onto CMS, pseudo first-order, pseudo second-order and intraparticle diffusion model were used to correlate the experimental data. The values of k_1 , q_{eq} and correlative coefficients of pseudo first-order model (before 120 minutes) are listed in Table 2. Although the first-order model gives extremely high correlative coefficients (>0.98), a large difference of equilibrium adsorption capacity (q_e) between the experiment and calculation was observed, which indicates a non-ideal fit to the experimental data.

The rate constant k_2 , the q_e value and correlative coefficient R^2 of pseudo-second order kinetics under different temperatures were calculated from the linear plots of t/q_t against t (not shown) and the results given in Table 2. Correlative coefficients (>0.95) and the calculated q_e values also reveal a poor fit to the experimental data.

The possibility of intraparticle diffusion cannot be overlooked because of the long adsorption equilibrium time in our experiments. For obvious illustration of this, an intraparticle diffusion model was proposed to describe the adsorption process (Fig. 4). The time dependence of q_t in Fig. 4 could present two straight lines which could be well fitted linearly. The multi-linearity suggested that the intraparticle diffusion was dominant in MG adsorption. The q_t in the

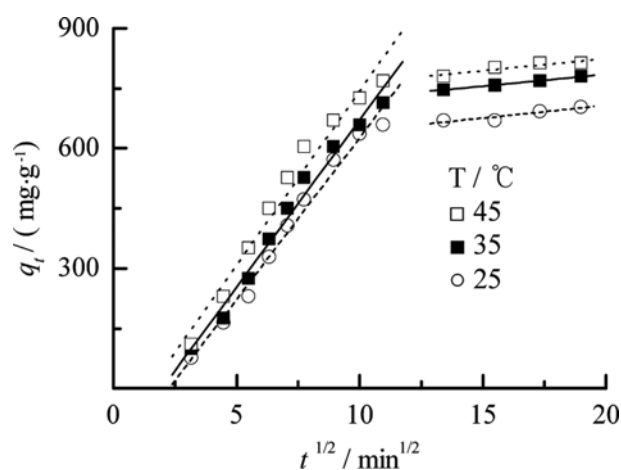


Fig. 4. Intra-particle diffusion model plots at different initial concentrations.

first portion showed a rapid increase with time, which was attributed to the rapid external diffusion of dyes to the surface of CMS. The second portion corresponded to the intraparticle diffusion effect. The values of k_{p1} , C_1 and correlative coefficients are also shown in Table 2. The correlation coefficients for the intraparticle diffusion model were all greater than 0.95. However, the linear plots do not pass through the origin of coordinates, which indicates that the intraparticle diffusion was not the sole rate-controlling step [10,14,24].

6. Comparison of the q_{max} of Various Adsorbents

Batch experiments were carried out in two conical flasks (150 mL, containing 0.01 g of CMS and 0.01 g of unmodified sawdust separately) filled with 100 mL of MG solutions with the concentration of 100 $\text{mg} \cdot \text{L}^{-1}$ at 25 °C for 6 h. The flasks were agitated on a shaker at 150 rpm constant shaking rate. The loading capacity was

Table 3. Comparison of adsorption capacities of various adsorbents for MG

Absorbent	Langmuir q_{max} (mg·g ⁻¹)	T (°C)	References
Triethylamine modified sawdust	826.45	45	Present work
Nano-iron oxide-loaded alginate microspheres	2.3	25	[25]
Macrophyte alligator weed	185.5	20	[26]
HP-3 de-inking paper sludge HP-3	982	-	[27]
RT-3 organic sludge RT-3	435	-	[27]
Mesoporous carbon	476.1	25	[28]
MCM-48	158.7	25	[29]
Activated carbon	222.2	30	[29]
Neem sawdust	4.35	25	[30]
Bentonite clay	7.72	30	[13]
Rattan sawdust	62.71	30	[31]
Carbon nanotube	142.9	25	[32]

determined to be 94.0 mg·g⁻¹ for unmodified sawdust and 697.8 mg·g⁻¹ for CMS. The capacity of CMS for MG was improved by 632.98% compared to that of the unmodified sawdust under the same adsorption conditions.

A list showing the maximum adsorption capacity of different materials for the adsorption of MG from its aqueous solution is given in Table 3. It was observed that the adsorption capacity of CMS for MG was comparable to other low-cost adsorbents. This provides strong evidence for the potential of CMS in technical applications of toxic cationic dye removal from aqueous solutions.

CONCLUSIONS

The adsorption of malachite green (MG) dye onto CMS as a novel adsorbent was carried out in batch mode. The effects of different operating parameters such as pH, contact time, initial MG concentration were evaluated. The results of present study indicated 5.05 of the optimal pH, 5 h to reach adsorption equilibrium, and increasing adsorption capacity with increasing temperature. Equilibrium data were correlated with Langmuir and Freundlich equations. Based on correlative coefficients, the experimental data followed the Freundlich isotherm. Kinetics reveal that the adsorption process of malachite green on sawdust tended to be controlled simultaneously by film mass transfer and by intra-particle diffusion, accompanied with chemical reactions. The results indicated CMS can be used as an effective adsorbent for dye removal.

ACKNOWLEDGEMENT

The work was supported by the Project Foundation of Chongqing Innovative Research Team Development in University (KJTD201020) and by the Project Foundation of Environmental Pollution Control Technology Innovative Team.

REFERENCES

1. M. F. Attallah, I. M. Ahmed and M. Hamed Mostafa, *Environ. Sci. Pollut. Res.*, **20**(2), 1106 (2013).
2. E. K. Mitter, G. C. Santos, E. J. R. Almeida, L. G. Morao, H. D. P. Rodrigues and C. R. Corso, *Water Air Soil Pollut.*, **223**(2), 765 (2012).
3. R. Ansari, B. Seyghali, A. Mohammad-khah and M. A. Zanjanchi, *J. Surfact Deterg.*, **15**(5), 557 (2012).
4. C. Shamik and D. S. Papita, *Environ. Sci. Pollut. Res.*, **20**, 1050 (2013).
5. P. M. K. Reddy, K. Krushnamurthy, S. K. Mahammadunnisa, A. Dayamani and Ch. Subrahmanyam, *Int. J. Environ. Sci. Technol.*, **12**(4), 1363 (2015).
6. F. Ferrero, *Clean Technol. Environ. Policy.*, DOI:10.1007/s10098-015-0908-y.
7. A. A. Olajire, A. A. Giwa and I. A. Bello, *Int. J. Environ. Sci. Technol.*, **12**(3), 939 (2015).
8. D. P. Tiwari, S. K. Singh and N. Sharma, *Appl. Water Sci.*, **5**(1), 81 (2015).
9. A. Mittal, V. Thakur and V. Gajbe, *Environ. Sci. Pollut. Res.*, **20**, 260 (2013).
10. X. Han, X. Niu and X. Ma, *Korean J. Chem. Eng.*, **29**(4), 494 (2012).
11. C. T. Weber, E. L. Foletto and L. Meili, *Water Air Soil Pollut.*, **224**(2), 1427 (2013).
12. G. H. S. Mokri, N. Modirshahla, M. A. Behnajady and B. Vahid, *Int. J. Environ. Sci. Technol.*, **12**(4), 1401 (2015).
13. S. S. Tahir and N. Rauf, *Chemosphere*, **63**(11), 1842 (2006).
14. S. Yinghua, L. Yi, C. Shengming, X. Hui and L. Yanran, *Fresenius Environ. Bull.*, **23**(4), 1074 (2014).
15. M. Saeed, R. Nadeem and M. Yousaf, *Int. J. Environ. Sci. Technol.*, **12**(4), 1223 (2015).
16. M. T. Yagub, T. K. Sen and M. Ang, *Environ. Earth Sci.*, **71**(4), 1507 (2014).
17. S. Lagergren, *Kungl. Svenska Vetenskapsakademiens Handlingar.*, **24**, 1 (1898).
18. Y. S. Ho and G. McKay, *Process. Biochem.*, **34**, 451 (1999).
19. W. J. Weber and J. C. Morriss, *J. Sanit. Eng. Div.*, **89**, 31 (1963).
20. X. Tang, Y. Li, R. Chen, F. Min, J. Yang and Y. Dong *Korean J. Chem. Eng.*, **32**(1), 125 (2015).
21. I. Bouaziz, C. Chiron and R. Abdelhedi, *Environ. Sci. Pollut. Res.*, **21**(14), 8565 (2014).
22. S. Sadaf and H. N. Bhatti, *Clean Techn Environ. Policy.*, **16**(3), 527 (2014).
23. X. X. Hou, Q. F. Deng and T. Z. Ren, *Environ. Sci. Pollut. Res.*,

- 20(12), 8521 (2013).
24. S. Dağdelen, B. Acemioğlu, E. Baran and O. Kocer, *Water Air Soil Pollut*, **225**, 1899 (2014).
25. A. Soni, A. Tiwari and A. K. Bajpai, *Res. Chem. Intermed.*, (Published online: 18 Jan 2013).
26. X. Wang, *Water Air Soil Pollut*, **206**(1), 215 (2010).
27. M. Ana, B. Sandra, S. Antonio, A. Méndez, S. Barriga, A. Saa and G. Gascó, *J. Therm. Anal. Calorim.*, **99**(3), 993 (2010).
28. M. Anbia and A. Ghaffari, *J. Iran Chem. Soc.*, **8**(Suppl.), S67 (2011).
29. R. Malik, D. S. Ramteke and S. R. Wate, *Waste Manage.*, **27**(9), 1129 (2007).
30. S. D. Khattri and M. K. Singh, *J. Hazard. Mater.*, **167**(1/2/3), 1089 (2009).
31. B. H. Hameed and M. I. El-Khaiary, *J. Hazard. Mater.*, **159**(2/3), 574 (2008).
32. M. Shirmardi, A. H. Mahvi, B. Hashemzadeh, A. Naeimabadi, G. Hassani and M. V. Niri, *Korean J. Chem. Eng.*, **30**(8), 1603 (2013).